Mechatronic design & adaptive control of a lower limb prosthesis

Mazumder, Aniket; Carloni, Raffaella

Published in:
2020 8th IEEE International Conference on BiomedicalRobotics and Biomechatronics (BioRob)

DOI:
10.1109/BioRob49111.2020.9224340

Publication date:
2020

2020 8th IEEE International Conference on Biomedical
Robotics and Biomechatronics (BioRob)
New York, USA. Nov 29 - Dec 1, 2020

Mechatronic Design & Adaptive Control of a Lower Limb Prosthesis

Aniket Mazumder and Raffaella Carloni

Abstract— **Lower limb prostheses have undergone significant developments in the last decades. However, there are several areas that have a scope for improvement through simplifications in the mechatronic design as well as in the control architecture. This paper focuses on the mechatronic design of a powered transtibial prosthesis and on the implementation of a control architecture, which is based on an adaptive frequency oscillator method that makes use of one inertial measurement unit. The control is capable of providing a positive push-off power to the prosthesis during level-ground walking and of adapting the response of the prosthesis to different walking speeds. The control architecture has been implemented and validated on a 3D printed prototype of a transtibial prosthesis. The experimental results show that the ankle joint can mimic the angle of a healthy subject with a root mean square error of 2.9° and that the gait transitions are tracked within two gait cycles.**

I. INTRODUCTION

Over the last couple of decades, lower limb prostheses have been the focus of several universities and research laboratories. Significant progress in this field has been made by researchers at Vanderbilt University [1] [2] [3], MIT [4] [5] [6], Rehabilitation Institute of Chicago [7] [8], etc. to name a few prominent ones. However, the pursuit of the ideal prosthesis might often lead to an increase in the complexity of mechanical design and control architecture. For example, the choice of an actuation system with series-parallel elastic actuators may decrease the overall size and power requirement from the active element but might also introduce a layer of complexity as compared to a direct drive system. Furthermore, a mechanically coupled knee-ankle system as done in Walkmech [9] [10] [11] [12] or Cyberleg-α [13] [14] might improve the overall efficiency of the system, but it might also reduce the versatility of the prosthesis for its use in diverse environments. Similarly, a control system that depends on multiple sensors placed externally on an amputee e.g., EMG's, Inertial Measurement Units(IMU's), etc, may interfere with the comfort of the amputee leading to a lack of adoption of the system as a whole. Again a system that uses multiple sensors internally, e.g., load-cells and IMU's have higher chances of failure. All these factors combined might often lead to a system that is complex in operation and lacks reliability.

Thus a system that is mechanically simple and employs an accordingly designed control system might be needed. One way of achieving this is through the use of adaptive central pattern generators first discussed by Righetti et al. [15] [16] to generate coordinated control signals for the actuation elements of the devices. Since several aspects of human movement walking, running, etc are cyclic, this approach has been used in the past to provide rehabilitation and assistive training to patients with upper and lower limb impairments [17]. There have been a few cases as shown by Torrealba et al. [18] and Ronsse et al. [19] where the approach has also been aimed at control of a prosthetic leg, however, the focus of these has been mainly to check the validity of the approach for the aforementioned application.

One aspect of functionality that is beneficial to have in an active lower limb prosthesis is the capability of having a dynamic response to changing walking speeds. This current work thus focuses on building from the ground up a mechanically simple, anthropomorphically similar prosthetic leg with an accompanying central pattern generator based adaptive control system that uses one single IMU to track the gait phase throughout the variations in walking speeds. The use of reference signals from just one IMU placed externally addresses the issue of complexity in the control system and through the use of an Adaptive Frequency Oscillator (AFO) algorithm [17] is capable of responding to changing gait patterns.

The remainder of the paper is organized as follows. In Section II, a detailed description of the steps followed in the mechatronic design of the lower limb prosthetic and in the implementation of the control system is provided. The results obtained on performing tests with the set-up have been presented and discussed in Section III. Finally, concluding remarks are drawn in Section IV.

II. METHODOLOGY

Building a prosthetic leg mainly consists of two parts: the design of the mechanical system and the design of the control system. Although these parts are often treated separately, it can be beneficial to consider them together, as it has been done in this work. This approach helps in getting a holistic idea of the system. In the following sections, the mechatronic design and the adaptive control architecture are presented.

A. Mechatronic Design

The prosthesis has been designed with two degrees of freedom, one each at the knee and the ankle. Functionality with simplicity was emphasized over complexity, hence the ankle was designed to allow at least 10° of dorsiflexion and 5° of plantar-flexion which is in line with normal human ankle range for level-ground walking. A ready-made foot

This work was supported by the European Union's Horizon 2020 Research and Innovation Program under grant agreement number 780871.

The authors are with the Faculty of Science and Engineering, Bernoulli Institute for Mathematics, Computer Science and Artificial Intelligence, University of Groningen, The Netherlands. {a.mazumder, r.carloni}@rug.nl

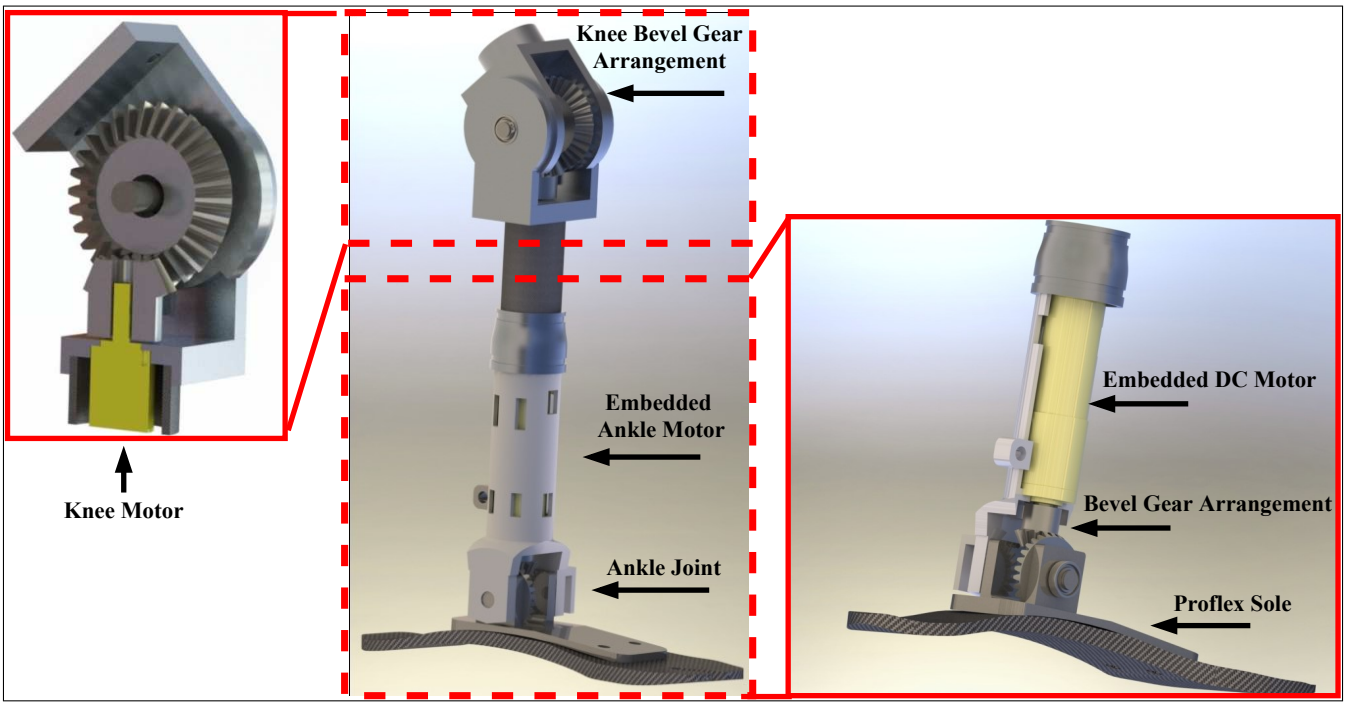

Fig. 1. 3D render of the designed prosthetic system. The cut away at the ankle section shows the embedded actuator placed within the shank of the prosthesis.

blade namely Ossur's Proflex® (Össur hf., Iceland, www.ossur.com) was attached to the ankle joint using a custom made connector to complete the foot design. The knee has been designed keeping in mind a range of motion of at least 90° in the sagittal plane allowing for knee flexion during sit to stand transition. These ranges are in line with knee angles for a healthy human gait as mentioned in Winter et.al [20]. An extra $-5°$ of knee hyperextension was allowed to help lock the knee in the stance rollover phase. The hyperextension also helps stabilize the knee during the weight-bearing phase. The axis of the knee joint was strategically placed behind the load line of the knee to assist in the stance hyper-extension phase of the gait cycle like a conventional passive prosthesis. The movements in both the joints were achieved by the use of a bevel gear mechanism that allowed concealment of the actuators within the shank of the prosthesis. Fig. 1 shows the 3D rendering of the complete lower limb prosthesis and the details of the bevel gear mechanism at the knee and ankle joints. The 3D drawings for all parts were made using Solidworks (Dassault Systèmes, France, www.solidworks.com) prototyping software.

Once the part modeling was satisfactory, finite element analysis of the parts was performed to verify the factor of safety for static and cyclic loading. To keep weight in check with reasonable strength most parts were conceived to be in carbon fibre and other aluminium and steel alloys. Further minimization of the weight of the designed prosthesis was possible though multiple topology optimizations allowing for a reduction in mass while preserving the load-bearing capability of the system.

The gear ratio for the ankle joint was calculated by using biomechanical data of healthy subject in [20] as a reference for the maximum angular velocity of the ankle joint. The nominal speed of the ankle motor reduced by the total ankle gear ratio including external bevel gears matched the peak ankle joint angular velocity. The knee gear ratio was chosen to increase the speed of the driven knee actuator to produce a higher voltage allowing for higher energy harvesting capability to improve the overall energy efficiency of the system.

For the ankle section, a Maxon RE30, 60 Watt (Maxon Group, Switzerland, www.maxongroup.com) brushed DC actuator coupled with a $67:1$ internal planetary gear head and $3:1$ external spur gears were used. The actuator was chosen keeping in mind the size and weight of the ankle system and was embedded internally within the tibia section to preserve the anthropomorphic shape of the lower leg. The selected motor coupled with the gear set can provide peak torques of 50 Nm in burst mode. This value is about 65% of the peak value [20] required for push-off from a healthy human ankle for the entire gait cycle. However, the actuator can be strategically powered during the beginning and end of the ankle push-off phase to provide an assistive push off to the user. Since the ankle joint is backdriveable, the inclusion of end stops in the design ensures that the ankle is locked between the limits mentioned earlier. For the knee, a smaller Maxon DCX actuator coupled with planetary gearhead with a reduction of $243:1$ was used. The knee section was connected to the ankle section using a standard prosthetic connector. The overall weight of the prosthesis is 2.4 kg without batteries. With a 24 V battery pack, it should weigh close to 3kg.

B. Control Architecture Design

The hardware for the control system of the prosthesis consists of a PIC32 200MHz micro-controller interfaced with the sensors using the I2C protocol. This was chosen to keep in mind the extensibility of the work in the future. Subsequently, a high power motor driver and current sensor from Pololu (Pololu Corporation, USA, `www.pololu.com`), the MPU 9250- 9 DOF IMU (SparkFun, USA, `www.sparkfun.com`) and a magnetic encoder from AMS AS5600L systems (AMS AG, Austria, `www.ams.com`) for contact-less absolute position sensing formed the backbone of the control system for the prosthesis. Data were sampled from the position sensors and IMU at a frequency of 200 Hz whereas the current sensors were sampled at a frequency of 2 KHz. Power was supplied using a lab bench power supply supplying 24 V to the actuator. The encoder was mounted on custom-designed encoder mounts placed around the shaft ends of the knee and ankle. The IMU for the control system is placed proximal to the body above the knee joint. This placement is chosen to get a better estimate of the movement of the upper body instead of the lower leg, which in turn can give us better estimates of the tendency of motion of the amputee. The placement also avoids noise that can be introduced when the IMU is placed on the distal section of the lower leg.

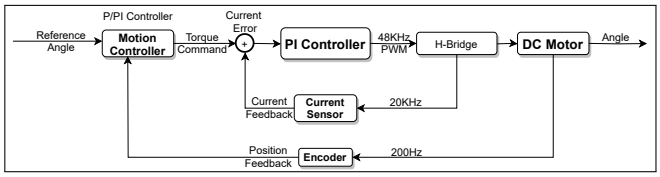

Fig. 2. Low level control system for the prosthesis.

Algorithm 1: Gait Adaptation Algorithm

Result: Get estimated gait phase

Initialize: $M \leftarrow 3; \nu \leftarrow 1; \epsilon \leftarrow 80; f_{min} \leftarrow 0.5;$

$$ZeroValues: Y_0 \leftarrow \begin{bmatrix} \phi_0 \\ \omega_0 \\ \alpha_0 \\ \beta_0 \end{bmatrix} = \begin{bmatrix} 0_{M\times 1} \\ 2\pi f_{min} \\ 0_{M\times 1} \\ 0_{1\times 1} \end{bmatrix}_{(2M+2)\times 1}$$

$a_z \leftarrow$ IMU ;
/* get accleration from IMU */

$A_{des}(t) \leftarrow a_y - 9.8;$
/* remove acceleration due to gravity */

$A_{est}(t) \leftarrow \beta_{t-1} + \sum_{i=1}^{M} \alpha_{t-1}(i) sin(\phi_{t-1}(i));$
/* estimate acceleration */

$T(t) \leftarrow (A_{des} - A_{est});$
/* formulate teaching signal */

$$\begin{bmatrix} \dot{Y}_t(i) \\ \dot{Y}_t(M+1) \\ \dot{Y}_t(M+1+i) \\ \dot{Y}_t(2M+2) \end{bmatrix} = \begin{bmatrix} iY_{t-1}(M+1)+\epsilon T(t)cos(Y_{t-1}(i)) \\ \epsilon T(t)cos(Y_{t-1}(1)) \\ \nu T(t)sin(Y_{t-1}(i)) \\ \nu T(t) \end{bmatrix}$$

$Y_t \leftarrow \int \dot{Y}_t;$
/* integrate */

$Y_t(1) \leftarrow mod(Y_t(1), 4\pi)$

return $Y_t(1)$ & $Y_t(M+1)$
/* Return phase and frequency corresponding to human gait */

The control strategy of the prosthesis was based on a cascaded torque-position PI control approach with the inner current loop running at 20 KHz and outer position loop running at 200 Hz. Feedback for the control was taken from the current sensors and absolute encoders used around the joints of the system. The maximum torque commanded by the actuators was limited to prevent overheating in the actuators. Estimation of gait was done using an IMU through the use of an oscillator algorithm. The algorithm aimed to keep track of the changing gait speeds of the amputee. All codes were written in C and compiled using MPLAB XC32 compiler. The low-level control system for the setup has been detailed in Fig. 2.

The high-level control of the prosthesis keeps track of the changing gait of the amputee in real-time, using an AFO-based [15] [17] algorithm. The algorithm used M sinusoidal oscillators with parameters α, β, ω which controlled the amplitude, offset, and angular frequency and generated an estimated acceleration A_{est}. Here M is the minimum number of oscillators that are chosen to give a Fourier representation of the desired signal. A teaching signal T was then generated as a difference between the desired and the estimated acceleration. This teaching signal was used to alter the frequency of the oscillators in real-time using the differential equations set $\dot{Y}$ after initialization Y_0 as shown in Algorithm 1. For the AFO, ϵ, ν, and f_{min} formed the parameters controlling the coupling strength, learning factor, and the minimum frequency limit. Trials were made to choose these parameters to ensure rapid adaptation.

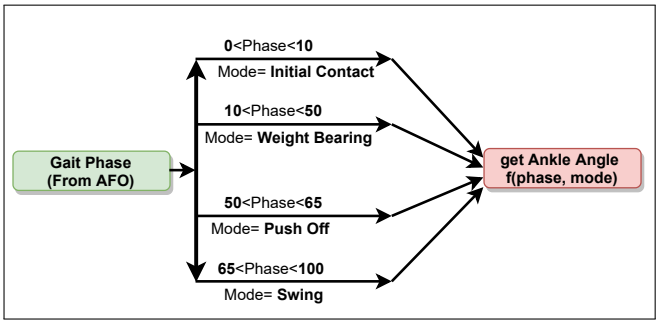

Fig. 3. State Machine for the prosthesis.The gait phase is obtained from the above mentioned algorithm and accordingly the state for the prosthesis is decided and fed into the controller.

To have an active response from the actuator while keeping track of the gait of the amputee, a state machine based on the changing gait phase obtained from the AFO was formulated. The state machine consisted of four parts of the

gait cycle which are Initial contact, weight-bearing, push-off, and swing. The goal of the state machine was to command a position to the actuator based on the gait phase information received from the IMU-based estimation algorithm. The gait phase decided the desired ankle angle through a linear fit of healthy human gait data divided into four sub-phases as shown in Fig. 3.

The first mode of the state machine is the initial contact phase that lasts for about 10% of the gait cycle. In this mode, the ankle prepares for impact and ends in a normal relaxed state of the ankle. Following the progression of gait into the second mode, the weight-bearing phase that lasts for about 40% of the gait cycle begins and ends with a plantar-flexion in preparation for push-off. The third mode or the push-off phase is the shortest phase which lasts for around 10% of the gait cycle with power transfer to the ankle. Here the position of the ankle changes from dorsiflexed to a plantarflexed state rapidly propelling the body forward. Subsequently, push-off is accompanied by the final mode or the swing phase that lasts for 40% of the gait cycle where the foot is dorsiflexed to maintain toe-clearance during the mid-swing. The mode curves for each of the four modes were obtained using a curve fit of healthy human gait data [20]. The choice of the breakpoints in the modes allowed for linear fit to be used for the purpose. Care was taken to ensure that the start and the end values of the curves between the modes match with one another. Linear fit also allowed a decrease in the complexity of calculations which were done in real-time on the embedded system.

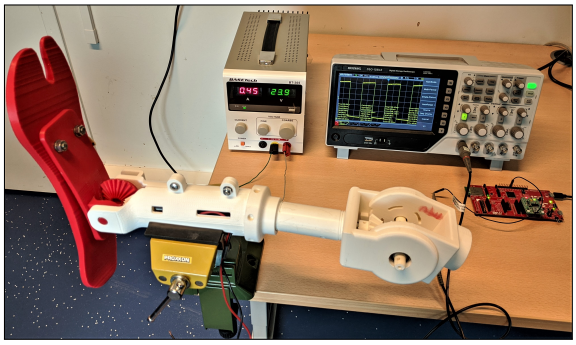

Fig. 4. Test setup used for testing the algorithms on the Prosthesis showing the PIC32 micro-controller, power supply and the scope.

III. Results and Discussions

Fig. 4 shows the test setup for the prosthetic system. The 3d printed prototype was held on a tabletop using a bench vice, while power was supplied to the system using a lab-bench power supply while being controlled through the microcontroller system. To test the response of the system, the IMU was perturbed vertically at regular intervals to generate an acceleration pattern that is similar to that of the human limb. The Z-axis of the IMU pointed in the direction opposite to that of the acceleration due to gravity 'g'. It must be mentioned that AFO algorithms can adapt to a varied range of repetitive signals based on a choice of parameters, and since human walking is a cyclic process generating repetitive signals along X, Y, and Z adaptation to each one of these directional accelerations would be possible using the same algorithm, provided the signal to noise ratio is sufficiently high.

The data from the sensors generated in real-time as a result of the experiments done using the prosthesis were directly logged onto a PC using a USB-UART communication bus. The results obtained using the test set-up are presented in Fig. 5 and Fig. 6.

Fig. 5 shows three subplots showing the results when a transition is made from a fast to slow and then back to fast walking mode. The zones in red represent a higher magnitude of accelerations which occurs during high-speed walking whereas the green zone represents a lower magnitude of acceleration representing slow walking. The first subplot in Fig. 5 shows the IMU vertical acceleration and the estimated acceleration generated by the AFO algorithm. The second subplot shows the phase of the first oscillator corresponding to the gait phase, while the third subplot shows the variation of ankle angle as a function of the gait phase and mode.

The phase of the first oscillator matched the gait phase of the teaching signal. Trials showed that at least two gait cycles were required for adaptation to reach acceptable levels. Initial tests showed that the real-life adaptation capability was limited to a window of frequencies and trials exceeding these limits show poor adaptation. Herein lies the need for concurrent algorithms that keep track of the gait phase. However, the frequencies of walking that lie between the ranges of slow to moderately fast walking fall well inside this range. These limits and the rate of adaptation can also be changed by changing the AFO parameters. Changing the weights for these parameters can also change the ranges for adaptation.

As can be seen in the figure, the transition from slow to fast and back was tracked by the oscillators satisfactorily and a corresponding gait phase and angles were generated by the prosthetic system. This adaptation of gait by the use of signals from a single IMU can reduce the overall number of sensors required for getting controlling a prosthetic leg. Accordingly, the problem of mode detection and switching of control parameters for different walking speeds can be handled by the algorithm in real-time.

Fig. 6 shows a comparison between the generated ankle angle and the reference human ankle angle obtained from tabletop studies performed on the model. As was mentioned earlier, the overall gait cycle was subdivided into four phases and a linear fit of the actual human data generated the reference angle during each mode. The curve fits for each mode along with the tracked ankle angle from the prosthesis, which has been shown in different colors in Fig. 6. An average of three consecutive gait cycles was considered to generate the figure.

The overall Root Mean Squared Error (RMSE) for the entire gait-cycle is $2.92°$. It can be seen that an acceptable level of a match exists between the reference angle and the actual generated angles of the prosthetic system for mode 1

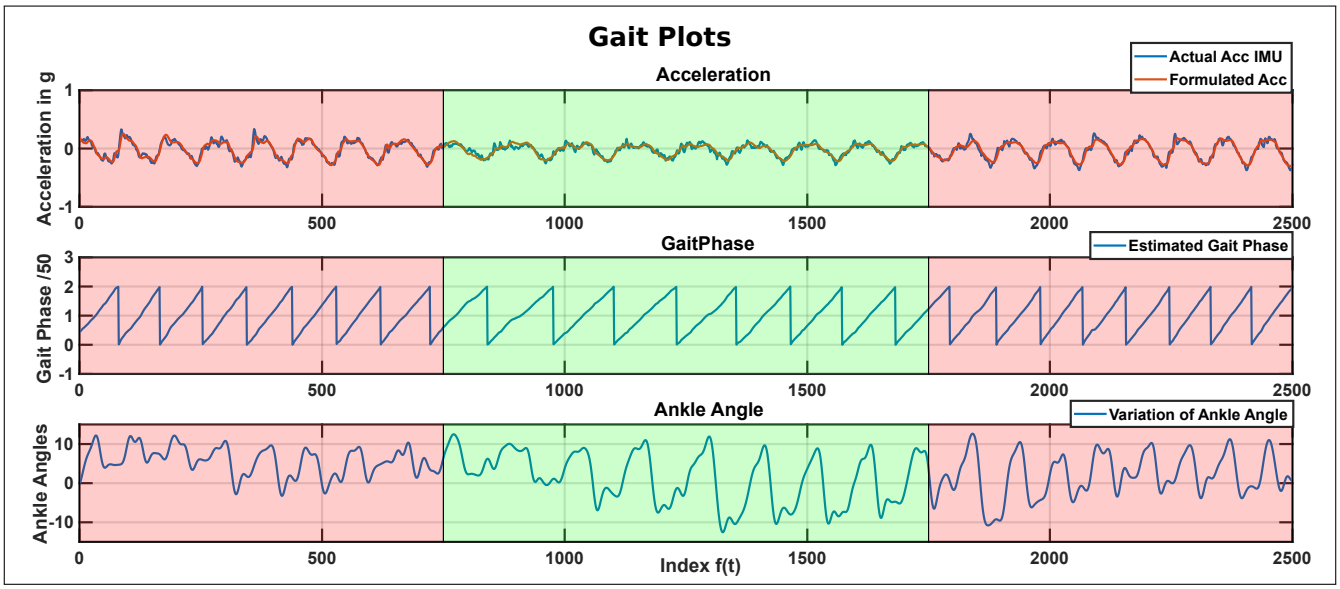

Fig. 5. Adaptation of gait with time. Red and green regions represent alternately occurring high and low magnitudes of acceleration.

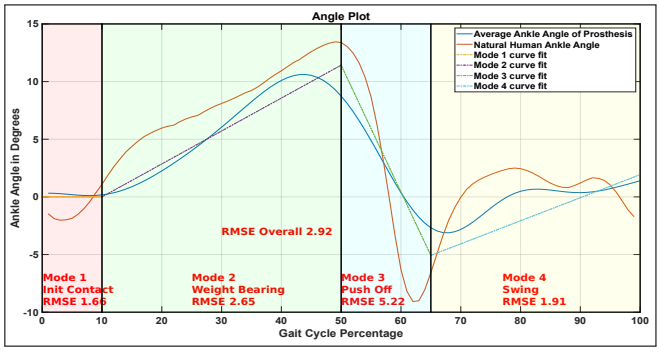

Fig. 6. Variation of reference ankle angle and generated ankle angle as a percentage of gait cycle. An average of three consecutive gait cycles have been used to generate the plots. The natural human ankle angles have been obtained from [20].

which is the initial contact phase of the gait cycle with an RMSE of 1.66° degrees. For mode 2 there is a deviation from the reference in the range of 1°-2° after the initial 10% with an RMSE of 2.66°. A large deviation exists in mode 3 with an RMSE of 5.23°. For mode 4 the deviation is larger during the initial phase, however, by the end of the gait cycle, there is a merging of actual and reference angles with an RMSE of 1.91°. The deviations in angles while transitioning between mode 2-3 and 3-4 can be attributed to high levels of angular accelerations occurring at the transition points due to the linear curve fit. Mathematically, these points suffer from the absence continuity of first and second derivatives leading to infinite velocities and accelerations. One way to remove these could be the use of higher-order curves for example cubic or a spline fit to generate the reference angles.

It must be mentioned that the current algorithm is aimed at tackling the issue of adapting the response of the prosthetic system during level-ground walking only. Although the knee actuator is included in the mechatronic design it has not been kept as a part of the current control system. With further modifications to the control system, the same algorithm might be used for ramp up and ramp down walking as well. Subsequently, to ensure reliable control using this technique, the current algorithm needs to be supplemented with additional abstractions that can take care of uncertainties ex:start-stop walk transitions, stumble recovery, etc that occur during the gait of an amputee. Once these factors are taken into account, the completeness of the control system may be verified.

IV. CONCLUSIONS

In this work, a prosthesis having the capability of adapting to changing gait was built. The prosthesis employed sensor feedback from only one IMU and is currently capable of adapting its response to changing gait speeds within two gait cycles, thus emphasizing the simplicity of the system. To broaden the application of the current system, algorithms that control response during gait initiation and termination needs to be designed and implemented into the system. Currently, the low-level control system features an interior current control loop cascaded with a position control loop. The response of the low-level control system may be improved by including a velocity control loop in between the current and position control loops. As the prosthesis is currently in the development phase, all tests were made on a lab bench. Subsequently, design changes shall incorporate control of knee actuator and power systems within the leg to perform subject tests. Furthermore, an improvement in the low and high-level controller through the use of a more robust control system with varying impedance or a hybrid position-torque control might be a better choice for the current application. All these possibilities shall be tested in the future.

ACKNOWLEDGMENT

The authors would like to thank Vishal Raveendranathan, doctoral candidate at the Bernoulli Institute for Mathematics, Computer Science, and Artificial Intelligence of the University of Groningen (The Netherlands), for the insightful discussions that have helped in this work. The authors would also like to extend their gratitude to Edsko E.E.G. Hekman, lecturer at the Department of Biomechanical Engineering of the University of Twente (The Netherlands), for his extremely valuable suggestions while finalizing the design of the prosthesis.

REFERENCES

[1] F. Sup, "A powered self-contained knee and ankle prosthesis for near normal gait in transfemoral amputees," Ph.D. dissertation, Vanderbilt University, 2009.

[2] F. Sup, A. Bohara, and M. Goldfarb, "Design and control of powered transfemoral prosthesis," *International Journal of Robotic Research*, vol. 27, no. 2, pp. 263–273, 2008.

[3] A. Bohara, "Finite state impedance-based control of a powered transfemoral prosthesis," Master's thesis, Vanderbilt University, 2006.

[4] S. Au, J. Weber, and H. Herr, "Powered ankle-foot prosthesis improves walking metabolic economy," *IEEE Transactions on Robotics*, vol. 25, no. 1, pp. 51–66, 2009.

[5] S. Au and H. Herr, "Powered ankle-foot prosthesis," *IEEE Robotics & Automation Magazine*, vol. 15, no. 3, pp. 52–59, 2008.

[6] S. Au, M. Berniker, and H. Herr, "Powered ankle-foot prosthesis," *Elsevier Neural Networks*, vol. 21, no. 4, pp. 654–666, 2008.

[7] M. Tran, L. Gabert, M. Cempini, and T. Lenzi, "A lightweight, efficient fully powered knee prosthesis with actively variable transmission," *IEEE Robotics and Automation Letters*, vol. 4, pp. 1186–1193, 2019.

[8] M. Cempini, L. Hargrove, and T. Lenzi, "Design, development, and bench-top testing of a powered polycentric ankle prosthesis," in *IEEE/RSJ International Conference on Intelligent Robots and Systems*, 2017, pp. 1064–1069.

[9] R. Unal, R. Carloni, E. Hekman, S. Stramigioli, and H. Koopman, "Conceptual design of an energy efficient transfemoral prosthesis," in *IEEE/RSJ International Conference on Intelligent Robots and Systems*, 2010, pp. 343–348.

[10] R. Unal, F. Klijnstra, B. Burkink, S. Behrens, E. Hekman, S. Stramigioli, and R. Carloni, "Modeling of WalkMECH: A fully-passive energy-efficient transfemoral prosthesis prototype," in *IEEE International Conference on Rehabilitation Robotics*, 2013, pp. 1–6.

[11] S. Behrens, R. Unal, E. Hekman, R. Carloni, S. Stramigioli, and H. Koopman, "Design of a fully-passive transfemoral prosthesis prototype," in *IEEE/EMBS International Conference of Engineering in Medicine and Biology Society*, 2011, pp. 591–594.

[12] R. Unal, R. Carloni, S. Behrens, E. Hekman, S. Stramigioli, and H. Koopman, "Towards a fully passive transfemoral prosthesis for normal walking," in *IEEE RAS/EMBS International Conference on Biomedical Robotics and Biomechatronics*, 2012, pp. 1949–1954.

[13] J. Geeroms, L. Flynn, R. Jimenez-Fabian, B. Vanderborght, and D. Lefeber, "Ankle-knee prosthesis with powered ankle and energy transfer for CYBERLEGs α-prototype," in *IEEE International Conference on Rehabilitation Robotics*, 2013, pp. 1–6.

[14] L. Ambrozic, M. Gorsic, J. Geeroms, L. Flynn, R. M. Lova, R. Kamnik, M. Munih, and N. Vitiello, "CYBERLEGs: A user-oriented robotic transfemoral prosthesis with whole-body awareness control," *IEEE Robotics & Automation Magazine*, vol. 21, no. 4, pp. 82–93, 2014.

[15] L. Righetti, J. Buchli, and A. Ijspeert, "Dynamic Hebbian learning in adaptive frequency oscillators," *Elsevier Physica D: Nonlinear Phenomena*, vol. 216, pp. 269–281, 2014.

[16] A. Oluwatosin, K. Djouani, and Y. Hamam, "Theory of adaptive oscillators: Mathematical principles and background," in *IEEE Africon Conference*, 2013, pp. 1–6.

[17] V. Vashista, M. Khan, and S. Agrawal, "A novel approach to apply gait synchronized external forces on the pelvis using A-TPAD to reduce walking effort," *IEEE Robotics and Automation Letters*, vol. 1, pp. 1118–1124, 2016.

[18] R. Torrealba, J. Cappelletto, L. Fermń, G. Fernández-López, and J. Grieco, "Cybernetic knee prosthesis: Application of an adaptive central pattern generator," *Kybernetes*, vol. 41, no. 1/2, pp. 192–205, 2012.

[19] R. Ronsse, N. Vitiello, T. Lenzi, J. van den Kieboom, M. Carrozza, and A. Ijspeert, "Adaptive oscillators with human-in-the-loop: Proof of concept for assistance and rehabilitation," in *IEEE RAS/EMBS International Conference on Biomedical Robotics and Biomechatronics*, 2010, pp. 668–674.

[20] D. Winter, *Biomechanics and motor control of human gait: normal, elderly and pathological*. University of Waterloo Press, 1991.